



Advanced imaging parameters improve the prediction of diffuse lower-grade gliomas subtype, IDH mutant with no 1p19q codeletion: added value to the T2/FLAIR mismatch sign

Min Kyoung Lee¹ · Ji Eun Park¹ · Youngheun Jo¹ · Seo Young Park² · Sang Joon Kim¹ · Ho Sung Kim¹

Received: 4 April 2019 / Revised: 11 July 2019 / Accepted: 25 July 2019 / Published online: 24 August 2019
© European Society of Radiology 2019

Abstract

Objectives A combination of T2/FLAIR mismatch sign and advanced imaging parameters may improve the determination of molecular subtypes of diffuse lower-grade glioma. We assessed the diagnostic value of adding the apparent diffusion coefficient (ADC) and cerebral blood volume (CBV) to the T2/FLAIR mismatch sign for differentiation of the IDH mutation or 1p/19q codeletion.

Materials and methods Preoperative conventional, diffusion-weighted, and dynamic susceptibility contrast imaging were performed on 110 patients with diffuse lower-grade gliomas. The study population was classified into three groups using molecular subtype, namely IDH mutation and 1p/19q codeletion (IDHmut-Codel), IDH wild type (IDHwt) and IDH mutation and no 1p/19q codeletion (IDHmut-Noncodel). T2/FLAIR mismatch sign and the histogram parameters of apparent diffusion coefficient (ADC) and normalised cerebral blood volume (nCBV) values were assessed. A multivariate logistic regression model was constructed to distinguish IDHmut-Noncodel from IDHmut-Codel and IDHwt and from IDHwt, and the performance was compared with that of single parameters using the area under the receiver operating characteristics curve (AUC).

Results Positive visual T2/FLAIR mismatch sign and higher nCBV skewness were significant variables to distinguish IDHmut-Noncodel from the other two groups (AUC, 0.88; 95% CI, 0.81–0.96). A lower ADC₁₀ was a significant variable for distinguishing IDHmut-Noncodel from the IDHwt group (AUC, 0.75; 95% CI, 0.62–0.89). Adding ADC or CBV histogram parameters to T2/FLAIR mismatch sign improved performance in distinguishing IDHmut-Noncodel from the other two groups (AUC 0.882 vs. AUC 0.810) or from IDHwt (AUC 0.923 vs. AUC 0.868).

Conclusions The combination of the T2/FLAIR mismatch sign with ADC or CBV histogram parameters can improve the identification of IDHmut-Noncodel diffuse lower-grade gliomas, which can be easily applied in clinical practice.

Key Points

- The combination of the T2/FLAIR mismatch sign with the ADC or CBV histogram parameters can improve the identification of IDHmut-Noncodel diffuse lower-grade gliomas.
- The multivariable model showed a significantly better performance for distinguishing the IDHmut-Noncodel group from other diffuse lower-grade gliomas than the T2/FLAIR mismatch sign alone or any single parameter.

Electronic supplementary material The online version of this article (<https://doi.org/10.1007/s00330-019-06395-2>) contains supplementary material, which is available to authorized users.

✉ Ji Eun Park
jjeunp@gmail.com

¹ Department of Radiology and Research Institute of Radiology, Asan Medical Center, University of Ulsan College of Medicine, 43 Olympic-ro 88, Songpa-Gu, Seoul 05505, South Korea

² Department of Clinical Epidemiology and Biostatistics, Asan Medical Center, University of Ulsan College of Medicine, Seoul, South Korea

- *The IDHmut-Noncodel type was associated with intermediate treatment outcomes; therefore, the identification of IDHmut-Noncodel diffuse lower-grade gliomas could be helpful for determining the clinical approach.*

Keywords Glioma · Magnetic resonance imaging · Diffusion magnetic resonance imaging · Isocitrate dehydrogenase

Abbreviations

AUC	Area under the receiver operating characteristics curve
DSC	Dynamic susceptibility contrast imaging
DWI	Diffusion-weighted imaging
ICC	Intra-class correlation coefficient
IDH	Isocitrate dehydrogenase
IDHmut-Codel	IDH mutant with 1p/19q codeletion subtype of diffuse lower-grade glioma
IDHmut-Noncodel	IDH mutant with no 1p/19q codeletion subtype of diffuse lower-grade glioma
IDHwt	IDH wild type of diffuse lower-grade glioma

Introduction

Diffuse lower-grade gliomas are traditionally classified as grades II and III based on morphological characteristics. However, recent findings led to a change in the classification of diffuse lower-grade gliomas according to phenotype and genotype [1, 2], based on mutation of the isocitrate dehydrogenase 1 and 2 (IDH1 and IDH2) genes and codeletion of chromosomes 1p and 19q [3, 4]. This molecular classification is more robust and useful for predicting prognosis [5], as patients with codeletion of 1p/19q show better treatment outcomes [6] and IDH1 mutation is predictive of longer survival [7]. The molecular classification of diffuse lower-grade glioma groups them into three categories: IDH wild type (IDHwt), IDH mutant with 1p/19q codeletion (IDHmut-Codel) and IDH mutant with no 1p/19q codeletion (IDHmut-Noncodel) [4]. IDHmut-Noncodel diffuse lower-grade gliomas have intermediate outcomes: they are more aggressive than IDHmut-Codel and have better outcomes than IDHwt diffuse lower-grade gliomas.

The difference between T2-weighted and fluid-attenuated inversion recovery (FLAIR) images was suggested as an indicator for the visual diagnosis of IDHmut-Noncodel diffuse lower-grade gliomas. The presence of the T2/FLAIR mismatch sign showed a positive predictive value of 100% in IDHmut-Noncodel diffuse lower-grade gliomas [4]. Visual assessment of the T2/FLAIR mismatch is a simple method that requires no further processing, and is therefore a clinically useful biomarker for the detection of IDHmut-Noncodel diffuse lower-grade gliomas. However, advanced MRI techniques, including diffusion-weighted imaging and dynamic

susceptibility contrast (DSC) MRI, are non-invasive techniques that can be used for classifying diffuse lower-grade gliomas [3, 8]. A meta-analysis showed a significant negative correlation between the apparent diffusion coefficient (ADC) and tumour cellularity in gliomas [9]. IDH mutations are associated with tumour angiogenesis, which can be detected using DSC MRI [8, 10]. IDHwt diffuse lower-grade gliomas are characterised by a high relative cerebral blood volume (rCBV) and low ADC value, whereas IDHmut-Codel gliomas have a lower rCBV and higher ADC [3]. Thus, the combination of ADC and CBV values may improve the characterisation of diffuse lower-grade gliomas.

There are currently few studies assessing the diagnostic performance of the combination of visual analysis and advanced imaging parameters for the molecular classification of diffuse lower-grade gliomas. Image-based approaches have potential as complementary diagnostic tools for the molecular classification of diffuse lower-grade gliomas, and could be valuable in planning the most appropriate treatment strategy, especially in cases of unresectable lesions in eloquent locations or in patients who cannot be operated on for medical problems. Although pathologic diagnosis remains the gold standard for differentiating diffuse lower-grade gliomas, sampling errors during biopsy or resection and intra- and inter-observer variations limit the reproducibility of this method in classifying molecular subtypes of diffuse lower-grade gliomas [11–13]. We hypothesised that combining the T2/FLAIR mismatch sign and advanced imaging parameters may improve the differentiation between IDHmut-Noncodel and other diffuse lower-grade gliomas. The present study examined the diagnostic value of the combination of quantitative MRI parameters and the T2/FLAIR mismatch sign for determining the molecular subtype of diffuse lower-grade gliomas.

Material and methods

Study population

The present study was a retrospective study conducted at Asan Medical Center between May 2015 and May 2017 that included 127 patients. The inclusion criteria were as follows: (1) a histopathologic diagnosis of diffuse lower-grade glioma; (2) obtained multiparametric MRI data. Molecular classification was performed using the 2016 WHO glioma classification guidelines based on IDH mutation and 1p/19q status [3]. Seventeen patients with IDH-mutant status but no 1p/19q

molecular classifications were excluded. The study enrolled 110 patients (56 men with a mean age of 47.4 ± 13.3 years; range, 19–82 years), including 45 WHO II and 65 WHO III diffuse lower-grade gliomas.

Molecular classification

IDH1 mutation status was determined by sequencing of codon 132 in the catalytic domain of IDH1 using standard genomic sequencing methods as previously described [14]. In brief, tumour DNA was isolated from frozen or formalin-fixed tissues using the DNeasy Blood and Tissue Kit (Qiagen). A 236-bp fragment that included codon 132 was amplified using the primers 5'-GCG TCA AAT GTG CCA CTA TC-3' and 5'-GCAAAA TCA CAT TAT TGC CAAC-3' to generate a 236-bp fragment. PCR products were sequenced by BigDye Terminator v1.1 (Applied Biosystems), and sequences were determined using a 3730 sequencer (Applied Biosystems).

The 1p/19q codeletion status was determined by fluorescence in situ hybridisation with specific probes for the 1p36 and 19q13 foci. Codeletion was defined as the deletion of > 50% of the nuclei examined for both 1p and 19q. The study population was divided into three groups according to the molecular characteristics: (1) IDHmut-Noncodel, (2) IDHwt and (3) IDHmut-Codel.

MRI acquisition protocol and preprocessing

All MR images were obtained on a 3-T unit (Achieva; Philips Medical Systems) using an 8-channel SENSE head coil. The brain tumour imaging protocol included the following sequences: T2-weighted imaging (T2WI), T1-weighted imaging (T1WI), FLAIR, DWI, DSC perfusion MRI and contrast-enhanced T1WI. The imaging parameters for DWI were as follows: image matrix, 256×256 ; repetition time (TR)/echo time (TE), 3000/56 ms and 4000/61.7 ms; diffusion gradient encoding, $b = 0$, 1000 s/mm^2 ; field of view (FOV), 24 cm; slice thickness/gap, 4 and 5 mm/2 mm; flip angle, 90° ; and acquisition time, 39 s.

For DSC perfusion MRI, a gradient-echo, echo-planar sequence was obtained during the administration of the standard dose (0.1 mmol/kg) of gadoterate meglumine (Dotarem; Guerbet). A preload of 0.01 mmol/kg gadoterate meglumine was given before the dynamic bolus, then the dynamic bolus was administered as a standard dose of 0.1 mmol/kg gadoterate meglumine (Dotarem; Guerbet) delivered at a rate of 4 mL/s using a MRI-compatible power injector (Spectris; Medrad). The bolus of contrast material was followed by a 20 mL bolus of saline, injected at the same rate. The imaging parameters for DSC perfusion MRI were as follows: image matrix, 128×128 ; TR/TE, 1808/40 ms; FOV, 24 cm; slice thickness/gap, 5/2 mm; flip angle, 35° ; and total acquisition time, 1 min and 54 s. Then, a post-contrast T1-weighted three-dimensional gradient-echo

sequence was acquired with the following parameters: image matrix, 512×512 ; TR/TE, 9.8/4.6 ms; FOV, 22–26 cm; slice thickness, 3 mm; and flip angle, 8° .

The ADC maps were calculated in b -values of 0 and 1000 s/mm^2 using a two-point estimate of signal decay: $\text{ADC} = \ln(S[b]/S[0])/b$, where b means b -value, and $S[0]$ and $S[b]$ indicate the signal intensities of images at b -values of 0 and 1000, respectively.

Commercial software (NordicICE; NordicNeuroLab) was used for processing the DSC images. The method of Weisskoff et al [15], which is used to correct T1 and T2 contamination, and its adaptation according to Boxerman et al [16] were used to perform CBV leakage correction. According to these correction methods, leakage was estimated from the deviation of each voxel from a non-leakage referent tissue response curve. The whole-brain rCBV was then calculated by numerical integration of the time concentration curve. For normalisation of the rCBV (nCBV), a neuroradiologist with 2 years of experience in neuro-oncology imaging manually selected a normal-appearing contralateral centrum semiovale (round region of interest (ROI), 4 mm diameter) and the mean intensity of the selected structure was used. CBV values were used for generating the nCBV in the contralateral ROI on a pixel-by-pixel basis.

Visual analysis for T2/FLAIR mismatch

The presence of T2/FLAIR mismatch was firstly assessed by two readers who are experienced neuroradiologists with 2 years (M.K.L.) and 5 years of experience (J.E.P.). The readers were blinded to the clinical history, histopathologic diagnosis and molecular classification. After anonymisation and data randomisation, the readers were given two image sets for each patient, which included FLAIR and T2WI. The T2/FLAIR mismatch sign was defined as a hyperintense signal on T2WI and a relatively hypointense signal on FLAIR images except for a peripheral hyperintense rim. The presence of T2/FLAIR mismatch was graded as follows: positive T2/FLAIR mismatch sign, equivocal and negative T2/FLAIR mismatch sign. Figure 1 shows examples of the three T2/FLAIR mismatch findings.

First, the readers examined 20 separate cases, and the intra-class correlation coefficient (ICC) for the assignment was measured. The ICC for the visual assessment of T2/FLAIR mismatch was 89, indicating excellent inter-reader agreement. Then, the readers reviewed the data in a conjoint manner to achieve a single reliable visual diagnosis. We chose this method because the conjoint reading mimics the real-world practice of radiologists. Also, we assumed that readers who were previously naive for this sign would perform similar analyses, given the high positive predictive value in the previous literature [4, 17]. Also, we calculated T2/FLAIR mismatch degree in quantitative analysis as follows.

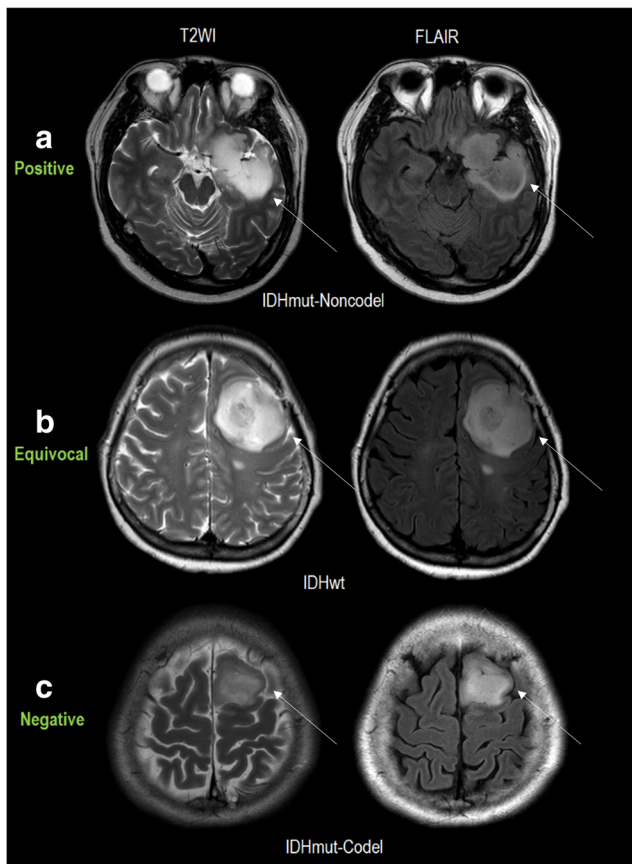


Fig. 1 Three cases of IDHmut-Noncodel diffuse lower-grade gliomas that were positive, equivocal and negative for the T2/FLAIR mismatch sign (arrows). **a** Positive T2/FLAIR mismatch sign in a left temporal lobe glioma with IDH mutation and no 1p/19q codeletion (IDHmut-Noncodel). **b** Equivocal T2/FLAIR mismatch sign in a left frontal glioma with IDH wild type (IDHwt). **c** Negative T2/FLAIR mismatch sign in a left frontal lobe glioma with IDH mutation and 1p/19q codeletion (IDHmut-Codel)

Quantitative analyses

For quantitative analysis, FLAIR images were registered to the ADC and nCBV maps using affine transformation with normalised mutual information as a cost function [18], six degrees of freedom and tri-linear interpolation. ROIs were drawn to encompass the entire hyperintense lesion on the FLAIR images and the enhancing solid portion in the cases with a contrast-enhancing tumour portion using MITK software (www.mitk.org; German Cancer Research Center). There were 61 patients (55.5%) with a contrast-enhancing tumour portion. The ROIs were drawn by an independent radiologist (S.Y.J.) with 3 years of experience in radiology and approved by an expert neuroradiologist (H.S.K.) with 20 years of experience in neuroradiology.

The quantitative analysis of T2/FLAIR mismatch sign was performed to support visual analysis as follows: first, ROI in the hyperintense tumour lesion on T2WI and FLAIR images. Then, another ROI was drawn in the contralateral normal-appearing white matter (CNWM) on both T2WI and FLAIR

images (Fig. 4). The T2/FLAIR mismatch degree was calculated using the following equation:

T2/FLAIR mismatch degree

$$= \frac{\text{T2 signal at tumour}}{\text{T2 signal at CNWM}} - \frac{\text{FLAIR signal at tumour}}{\text{FLAIR signal at CNWM}}$$

Histograms of ADC and CBV values were generated for the entire ROIs, with 100 equally spaced bins from the minimum and maximum pixel values. The cumulative histogram parameters of the 5th, 10th and 50th percentiles of ADC (ADC5, ADC10 and ADC50) and the mean ADC for the ROI were calculated. For nCBV, the cumulative histogram parameters of the 50th, 90th and 95th percentiles (nCBV50, nCBV90 and nCBV95) and mean nCBV were derived. Also, the entropy, skewness and kurtosis were further calculated. The histogram analysis was performed using a previously described strategy [19], which is less influenced by random statistical fluctuations.

Statistical analysis

Quantitative parameters were expressed as the mean \pm standard deviation. The Shapiro–Wilk test was used to determine normality. The Student *t* test and the Chi-square test were used to assess differences in demographic characteristics and parameters between the IDHmut-Noncodel and other diffuse lower-grade gliomas and between the IDHmut-Noncodel and IDHwt groups, and between IDHmutation groups (IDHmut-Noncodel and IDHmut-codel) and IDHwt group.

Diagnostic model Among clinical parameters of age and sex, T2/FLAIR mismatch, and ADC and CBV histogram parameters, significant variables in differentiating each group were selected using univariate and multivariate logistic regression analyses. The significant variables were used to construct a diagnostic model.

Analysis of diagnostic performance Receiver operating characteristics (ROC) curve analysis was performed to calculate the area under the ROC curve (AUC) between two readers and to determine the optimal cutoff. The diagnostic performance of the imaging parameters, including T2/FLAIR mismatch sign and ADC and nCBV values, was assessed independently for each reader. The optimal thresholds of the AUCs were determined by maximising the sum of the sensitivity and specificity values. The accuracy, sensitivity and specificity were calculated. Comparison of AUCs between single parameters (either T2/FLAIR mismatch sign or ADC/CBV parameter) and combined parameters was performed using DeLong’s test.

Multiple comparisons between four ADC and nCBV parameters were adjusted using Bonferroni correction. A *p* value < 0.05 was considered statistically significant. Statistical

analysis was performed using statistical software (R version R 3.3.3) and MedCalc.

Analysis of reproducibility The reproducibility analysis for histogram parameters was performed in 20 randomly selected patients. Inter-reader agreement for histogram parameters was assessed using the ICC.

Results

Of 110 participants, 19 were IDHmut-Noncodel, 45 were IDHwt and 46 were IDHmut-Codel (Table 1). After Bonferroni correction, patients with IDHmut-Noncodel group were younger ($p = 0.007$) than those with IDHwt. IDHwt patients had significantly more multilobar involvement ($p < 0.001$) than those with IDHmut-Codel and a higher rate of grade III gliomas ($p = 0.007$) than those with IDH mutation groups.

Comparison of ADC and nCBV parameters

Concordance of histogram parameters between two readers showed excellent agreement (ICC range, 0.963–0.998) (Supplementary Table 1). Table 2 summarises the differences in ADC and nCBV parameters between the groups. The IDHmut-Noncodel group had higher ADC parameters in ADC10 ($p = 0.001$) and ADC50 ($p = 0.007$) than the IDHmut-Codel group. The IDHmut-Noncodel group had higher ADC parameters of ADC5 ($p = 0.006$), ADC10 ($p =$

0.002), ADC50 ($p = 0.007$), mean ADC ($p = 0.015$) and ADC skewness ($p = 0.005$) and lower CBV parameters in nCBV95 ($p = 0.007$) and nCBV90 ($p = 0.008$) than the IDHwt group.

T2/FLAIR mismatch sign for predicting IDHmut-Noncodel

In the differentiation between IDHmut-Noncodel and other diffuse lower-grade gliomas, the AUC of the T2/FLAIR was 0.81 (95% confidence interval (CI), 0.73–0.90) with sensitivity, specificity and accuracy of 89.5%, 73.6% and 83.6%, respectively. The concordance between the qualitative T2/FLAIR mismatch sign and the quantitative degree was moderate ($R = 0.4654$, p value < 0.001).

Performance for distinguishing the IDHmut-Noncodel group from other diffuse lower-grade gliomas

In the univariate analysis, age ($p = 0.018$), visual and quantitative T2/FLAIR mismatch sign ($p < 0.001$ and 0.002), ADC histogram parameters ($p = 0.002$ –0.039), ADC5, ADC10, ADC50, mean ADC, ADC skewness, nCBV95 ($p = 0.020$), nCBV90 ($p = 0.017$) and nCBV skewness ($p = 0.018$) were significant predictors for distinguishing IDHmut-Noncodel from other groups (Table 3). Among image-based parameters, tumour enhancement was not a significant predictor of IDHmut-Noncodel ($p = 0.323$). In the multivariate analysis, visual T2/FLAIR mismatch sign ($p < 0.001$) and nCBV skewness ($p = 0.018$) remained significant predictors for diagnosing IDHmut-Noncodel.

Table 1 Demographics of the study population

	IDHmut-Noncodel ($n = 19$)	IDHwt ($n = 45$)	IDHmut-Codel ($n = 46$)	p	p^*	p^\dagger	p^+
Age (years)	40.74 ± 12.80	51.2 ± 14.02	46.54 ± 11.66	0.012	0.007	0.081	0.088
Male gender	9 (47.4%)	25 (55.6%)	22 (47.8%)	0.725	0.556	0.974	0.466
Grade							
II	13	12	20	0.007	0.001	0.069	0.003
III	6	33	26				
Location							
Frontal lobe	7	8	29				
Others	12	37	15				
Multilobar involvement	9 (47.4%)	30 (66.7%)	13 (28.3%)	0.001	0.153	0.143	< 0.001
Size (cm ²)	28.46 ± 16.67	30.00 ± 15.61	35.04 ± 21.91	0.271	0.808	0.245	0.172

IDHmut-Noncodel, IDH mutation and no 1p/19q codeletion; IDHwt, IDH wild type; IDHmut-Codel, IDH mutation and 1p/19q codeletion

P values are Bonferroni-corrected p values. p refers to the statistical significance among the three groups. p^* refers to the statistical significance for difference between IDHmut-Noncodel and IDHwt. p^\dagger refers to the statistical significance for difference between IDHmut-Noncodel and IDHmut-Codel. p^+ refers to the statistical significance for difference between IDHwt and IDHmut-Codel

Table 2 Comparison of ADC and CBV parameters between the IDH mutation with no 1p/19q codeletion group (IDHmut-Noncodel) and other LGGs (ANOVA)

	IDHmut-Noncodel (n = 19)	IDHwt (n = 45)	IDHmut-Codel (n = 46)	<i>p</i>	<i>p</i> [*]	<i>p</i> [†]	<i>p</i> ⁺
ADC (10 ⁻³ mm ² /s)							
ADC5	0.909 ± 0.094	0.829 ± 0.107	0.867 ± 0.079	0.007	0.006	0.066	0.054
ADC10	0.985 ± 0.112	0.881 ± 0.116	0.927 ± 0.081	0.001	0.002	0.023	0.033
ADC50	1.324 ± 0.206	1.143 ± 0.265	1.187 ± 0.127	0.007	0.010	0.002	0.316
Mean ADC	1.327 ± 0.190	1.175 ± 0.236	1.253 ± 0.157	0.016	0.015	0.111	0.064
ADC entropy	3.733 ± 0.549	3.559 ± 0.522	3.574 ± 0.447	0.414	0.236	0.227	0.887
ADC kurtosis	4.859 ± 4.612	5.722 ± 3.703	6.154 ± 5.914	0.625	0.432	0.398	0.678
ADC skewness	0.405 ± 0.818	1.002 ± 0.715	0.857 ± 1.110	0.063	0.005	0.115	0.462
nCBV (relative ratio)							
nCBV95	3.27 ± 1.08	4.29 ± 1.44	3.85 ± 1.24	0.016	0.007	0.080	0.119
nCBV90	2.58 ± 0.86	3.48 ± 1.29	3.11 ± 1.04	0.015	0.008	0.055	0.137
nCBV50	1.18 ± 0.39	1.53 ± 0.76	1.31 ± 0.46	0.065	0.061	0.273	0.103
Mean nCBV	1.42 ± 0.44	1.85 ± 0.75	1.59 ± 0.53	0.027	0.025	0.226	0.063
nCBV entropy	3.384 ± 0.363	3.448 ± 0.351	3.537 ± 0.376	0.225	0.513	0.137	0.246
nCBV kurtosis	8.385 ± 2.608	7.653 ± 2.720	6.702 ± 2.274	0.036	0.323	0.012	0.074
nCBV skewness	1.892 ± 0.363	1.653 ± 0.474	1.548 ± 0.500	0.030	0.054	0.008	0.304

IDHmut-Noncodel, IDH mutation and no 1p/19q codeletion; IDHwt, IDH wild type; IDHmut-Codel, IDH mutation and 1p/19q codeletion

P values are Bonferroni-corrected *p* values. *p* refers to the statistical significance among the three groups. *p*^{*} refers to the statistical significance for difference between IDHmut-Noncodel and IDHwt. *p*[†] refers to the statistical significance for difference between IDHmut-Noncodel and IDHmut-Codel. *p*⁺ refers to the statistical significance for difference between IDHwt and IDHmut-Codel

Based on visual T2/FLAIR mismatch, the AUC for distinguishing the IDHmut-Noncodel from other groups was 0.81 (95% CI, 0.73–0.90), with sensitivity, specificity and accuracy of 89.5%, 72.5% and 75.5%, respectively. The AUCs for nCBV skewness were 0.69 (95% CI, 0.57–0.81), respectively.

The combination of nCBV skewness and the visual T2/FLAIR mismatch sign significantly showed similar to better diagnostic performance compared with that of single parameters alone (AUC, 0.88; 95% CI, 0.80–0.96). Figure 2 shows a demonstrable case.

Performance for distinguishing the IDHmut-Noncodel group from IDHwt

For distinguishing IDHmut-Noncodel from IDHwt, age (*p* = 0.011), the ADC histogram parameters (*p* = 0.01–0.29), ADC5, ADC10, ADC50, mean ADC, ADC skewness, nCBV95 (*p* = 0.011), nCBV90 (*p* = 0.011) and CBV skewness (*p* = 0.018) were significant predictors in the univariate analysis. In the multivariate analysis, ADC10 (*p* = 0.043) was an independent predictor for distinguishing IDHmut-Noncodel from IDHwt (Table 3).

For differentiating between the IDHmut-Noncodel and IDHwt groups, the AUC of T2/FLAIR was 0.87 (95% CI, 0.78–0.96), with sensitivity, specificity and accuracy of

89.5%, 84.4% and 85.9%, respectively (Table 4). The AUCs for ADC10 were 0.75 (95% CI, 0.78–0.96), respectively.

Combination of the visual T2/FLAIR mismatch sign and ADC10 showed similar to better diagnostic performance (AUC, 0.92; 95% CI, 0.86–0.99) compared with that of the visual T2/FLAIR mismatch sign alone, whereas it was comparable with that of ADC 10 alone. Figure 3 shows a demonstrable case. Combination of the T2/FLAIR mismatch sign and nCBV90 improved the diagnostic performance (AUC, 0.89; 95% CI, 0.78–0.99; *p* = 0.57), although the difference was not significant.

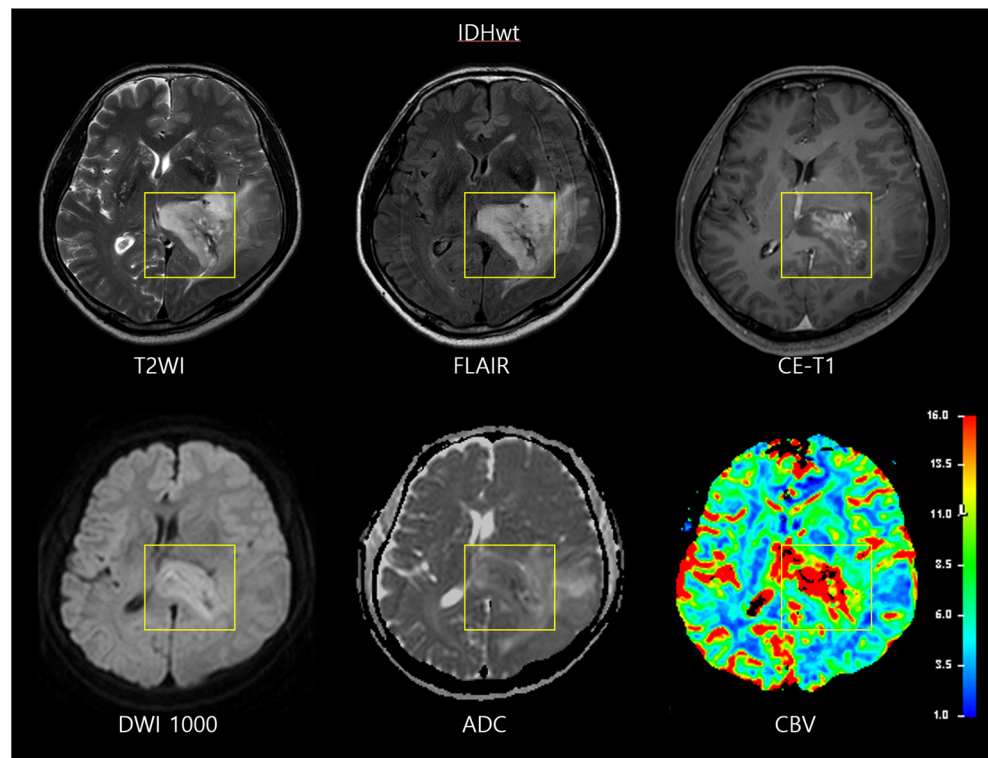
Performance for distinguishing between the IDH mutation groups and IDHwt

For distinguishing IDH mutation groups from IDHwt, age (*p* = 0.016), the ADC histogram parameters (*p* = 0.005–0.048), ADC5, ADC10, ADC50 and mean ADC, and the CBV histogram parameters (*p* = 0.018–0.037), nCBV95, nCBV90, nCBV50 and mean nCBV, were significant predictors in the univariate analysis. On multivariate logistic regression, for differentiating the IDH mutation groups from IDHwt, only visual T2/FLAIR mismatch sign (*p* < 0.001) was an independent predictor (Table 3).

Table 3 Univariate and multivariate logistic regression analyses for diagnosing IDH mutant, non-codetected group from others and IDH mutation

Variable	IDH mutant, non-codetected vs. others			IDH mutant, non-codetected vs. IDH wild group			IDH mutant group vs. IDH wild group		
	Univariate analysis	Multivariate analysis		Univariate analysis	Multivariate analysis		Univariate analysis	Multivariate analysis	
	β coefficient (95% CI)	p value	β coefficient (95% CI)	p value	β coefficient (95% CI)	p value	β coefficient (95% CI)	p value	β coefficient (95% CI)
Age	-0.048 (-0.089, -0.008)	0.018	-0.056 (-0.098, -0.013)	0.011	-0.038 (-0.069, -0.007)	0.016			
Sex	0.171 (-0.819, 1.161)	.735	0.329 (-0.747, 1.404)	0.549	0.316 (-0.448, 1.079)	0.419			
Visual T2/FLAIR mismatch	3.111 (1.575, 4.647)	0.0001	0.345 (0.196, 0.462)	<0.0001	0.634 (0.411, 0.827)	<0.0001	1.846 (0.904, 2.788)	0.0001	0.323 (0.276, 0.290)
Quantitative T2/FLAIR mismatch	1.670 (0.590, 2.750)	0.002	3.088 (1.260, 4.917)	0.001	0.003 (0.171, 2.206)	0.022	-0.010 (0.171, 2.206)	0.0001	0.323 (0.276, 0.290)
Contrast enhancement	0.003 (-0.003, 0.010)	0.323	0.004 (-0.004, 0.012)	0.372	0.006 (-0.004, 0.005)	0.882	0.006 (0.001, 0.010)	0.010	
ADC5	0.008 (0.002, 0.014)	0.014	0.009 (0.002, 0.015)	0.010	0.006 (0.001, 0.010)	0.010	0.006 (0.002, 0.010)	0.005	
ADC10	0.008 (0.003, 0.014)	0.004	0.009 (0.003, 0.015)	0.004	0.001 (0.00003, 0.002)	0.043	0.006 (0.002, 0.010)	0.005	
ADC50	0.003 (0.0005, 0.006)	0.017	0.004 (0.0003, 0.0060)	0.028	0.002 (0.00002, 0.005)	0.048	0.002 (0.00002, 0.005)	0.048	
Mean ADC	0.003 (0.0001, 0.005)	0.039	0.003 (0.003, 0.006)	0.029	0.003 (0.0006, 0.005)	0.014	0.003 (0.0006, 0.005)	0.014	
ADC entropy	0.681 (-0.329, 1.691)	0.186	0.627 (-0.404, 1.658)	0.526	0.252 (-0.523, 1.026)	0.524	0.252 (-0.523, 1.026)	0.524	
ADC skewness	-0.701 (-1.327, -0.075)	0.028	-1.229 (-2.147, -0.312)	0.009	-0.329 (-0.757, 0.0981)	0.131	-0.329 (-0.757, 0.0981)	0.131	
ADC kurtosis	-0.069 (-0.222, 0.084)	0.377	-0.063 (-0.220, 0.094)	0.431	0.002 (-0.077, 0.081)	0.955	0.002 (-0.077, 0.081)	0.955	
nCBV95	-0.659 (-1.214, -0.103)	0.020	-0.811 (-1.438, -0.184)	0.011	-0.357 (-0.664, -0.049)	0.023	-0.357 (-0.664, -0.049)	0.023	
nCBV90	-0.854 (-1.553, -0.156)	0.017	-1.016 (-1.798, -0.234)	0.011	-0.408 (-0.767, -0.050)	0.026	-0.408 (-0.767, -0.050)	0.026	
nCBV50	0.869 (-1.935, 0.198)	0.110	-1.048 (-2.166, 0.070)	0.066	-0.751 (-1.457, -0.045)	0.037	-0.751 (-1.457, -0.045)	0.037	
Mean nCBV	-1.006 (-2.075, 0.063)	0.065	-1.313 (-2.498, -0.127)	0.030	-0.816 (-1.495, -0.138)	0.018	-0.816 (-1.495, -0.138)	0.018	
nCBV entropy	-0.825 (-2.197, 0.547)	0.239	-0.523 (-2.068, 1.022)	0.507	0.337 (-0.713, 1.386)	0.530	0.337 (-0.713, 1.386)	0.530	
nCBV skewness	1.387 (0.235, 2.539)	0.018	0.155 (0.034, 0.303)	0.024	0.061 (-0.818, 0.774)	0.958	0.061 (-0.818, 0.774)	0.958	
nCBV kurtosis	0.174 (-0.012, 0.359)	0.067	0.101 (-0.098, 0.300)	0.320	-0.069 (-0.217, 0.079)	0.359	-0.069 (-0.217, 0.079)	0.359	

Fig. 2 Grade II glioma with IDH mutation and no 1p/19q codeletion (IDHmut-Noncodel) shows no definite diffusion restriction and a low CBV value with positive visual T2/FLAIR mismatch sign (square)



The AUC of visual T2/FLAIR mismatch for distinguishing between the IDH mutation groups and IDHwt was 0.69 (95% CI, 0.60–0.77) (Table 4).

Discussion

In the present study, we demonstrated the usefulness of quantitative measurement of ADC and CBV when used in combination with the T2/FLAIR mismatch sign for predicting the IDHmut-Noncodel molecular subtype. The combination of ADC and CBV histogram parameters, and the T2/FLAIR mismatch sign showed a trend to better performance for distinguishing the IDHmut-Noncodel group from other diffuse lower-grade gliomas and from IDHwt than the T2/FLAIR mismatch sign alone or any single parameter.

Among diffuse lower-grade gliomas, the IDH mutation groups showed a more favourable clinical outcome than the IDHwt group [20], and the IDHwt group showed the most aggressive clinical outcome and behaviour, similar to those of glioblastoma [4]. Among the IDH mutation groups, the IDHmut-Noncodel type shows intermediate treatment outcomes compared with the IDHmut-Codel type [4]; therefore, the identification of IDHmut-Noncodel diffuse lower-grade gliomas could be helpful for determining the clinical approach. The T2/FLAIR mismatch sign is a highly specific marker for identifying diffuse lower-grade gliomas, showing a PPV of 100% in both internal and external validation [4, 17]

without any false-positive cases. Although the T2/FLAIR mismatch sign showed good diagnostic performance for differentiating between IDHmut-Noncodel and other diffuse lower-grade gliomas, there were 10 false-positive cases and imperfect positive predictive values. On retrospective review, this occurred mainly due to background signal decrease on FLAIR mimicked internal signal decrease in IDHwt, while pronounced FLAIR signal decrease occurred in IDHmut-Codel type in a large cyst-like pattern [21]. The present results may demonstrate the real-world performance of the T2/FLAIR mismatch sign, as determined by consensus reading by neuroradiologists with 2 and 5 years of experience, which is a common clinical situation. The false-positive T2/FLAIR mismatch sign should be combined with quantitative imaging parameters to establish a more accurate, non-invasive molecular subclassification.

In addition, for evaluation of the T2/FLAIR mismatch sign, we used both qualitative and quantitative approaches. In the univariate logistic regression, both qualitative and quantitative T2/FLAIR mismatch signs were significant indicators for distinguishing the IDHmut-Noncodel from other groups. The two approaches used to assess the T2/FLAIR mismatch sign showed a moderate concordance coefficient ($R = 0.4654$, $p < 0.001$); therefore, both approaches could be used for the detection of IDHmut-Noncodel. However, the visual T2/FLAIR mismatch sign is simpler to use as a parameter than the quantitative T2/FLAIR mismatch sign.

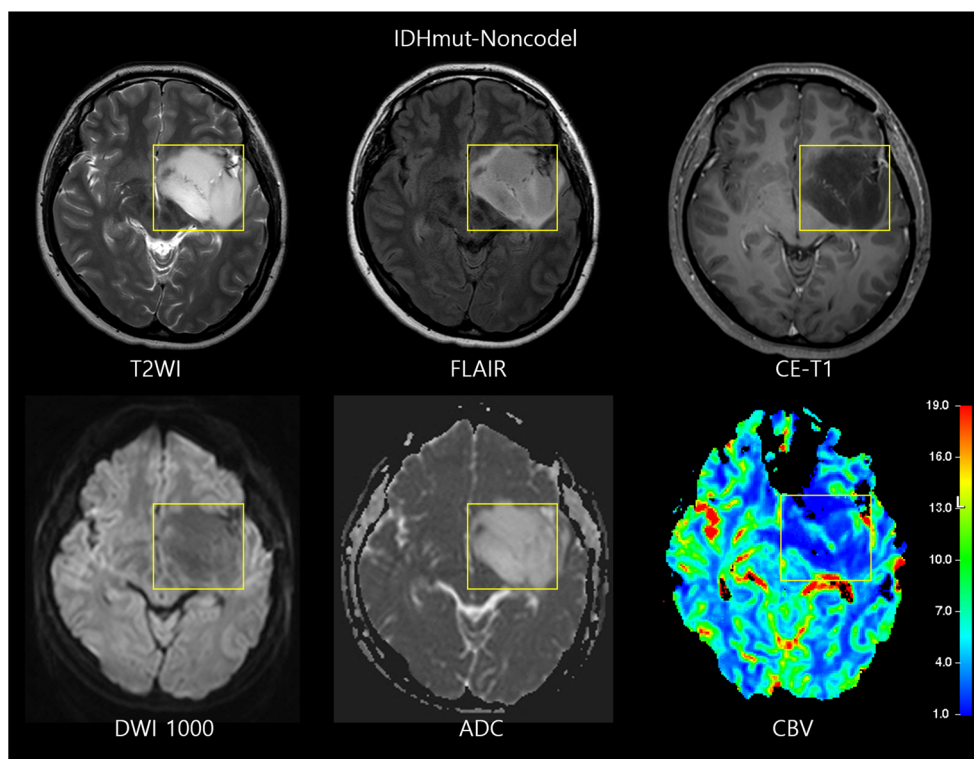
Table 4 Comparison of diagnostic performance for distinguishing the IDH mutation with no 1p/19q codeletion group (IDHmut-Noncodel) from other diffuse grade II/III gliomas and the IDH mutation from IDH wild type (IDHwt)

IDHmut-Noncodel vs. other LGGs ($n = 110$)	AUC	Sensitivity	Specificity	Accuracy
Combined model (visual T2/FLAIR mismatch and nCBV skewness)	0.882 (0.801, 0.964)	89.5	80.2	81.8
Visual T2/FLAIR mismatch	0.810 (0.725, 0.895)	89.5	72.5	75.5
nCBV skewness	0.690 (0.573, 0.807)	84.2	59.3	63.6
IDHmut-Noncodel vs. IDHwt ($n = 64$)	AUC	Sensitivity	Specificity	Accuracy
Combined model (visual T2/FLAIR mismatch and ADC 10)	0.923 (0.855, 0.992)	89.5	86.4	87.3
Visual T2/FLAIR mismatch	0.868 (0.778, 0.957)	89.5	84.1	85.7
ADC 10	0.751 (0.617, 0.886)	84.2	63.6	69.8
IDHwt vs. IDHwt ($n = 110$)	AUC	Sensitivity	Specificity	Accuracy
Visual T2/FLAIR mismatch	0.686 (0.604, 0.767)	53.0	84.1	65.5

Numbers in parentheses are 95% confidence intervals. *AUC*, area under the receiver operating characteristics curve
T2/FLAIR indicates positive for the T2/FLAIR mismatch sign

Quantitative ADC and CBV analyses were previously used for predicting IDHwt, whereas their application to the identification of the IDHmut-Noncodel group is relatively unknown. The present findings are consistent with those of previous studies showing that IDHmut-Noncodel diffuse lower-grade gliomas have significantly higher ADC values and lower nCBV values than IDHwt diffuse lower-grade gliomas [3, 8, 22, 23]. The higher ADC values in the IDHmut-Noncodel group can also be explained by the absence of 1p/19q codeletion that gliomas with 1p/19q

codeletion are more homogeneous and have smaller oedematous areas and larger cellular areas than IDHmut-Noncodel diffuse lower-grade gliomas [24]. The ADC value is an indicator of tumour cellularity [9], and a high ADC value indicates lower cellularity in the IDHmut-Noncodel group. The homogeneously high T2 signal intensity in this group with a positive T2/FLAIR mismatch sign may be reflective of lower cellularity; the ADC10 value improves the accuracy of the visual T2/FLAIR mismatch findings in the IDHmut-Noncodel group, and the ADC and CBV

Fig. 3 Grade III glioma with IDH wild type (IDHwt) shows diffusion restriction and an increased CBV value with positive visual T2/FLAIR mismatch sign (box)

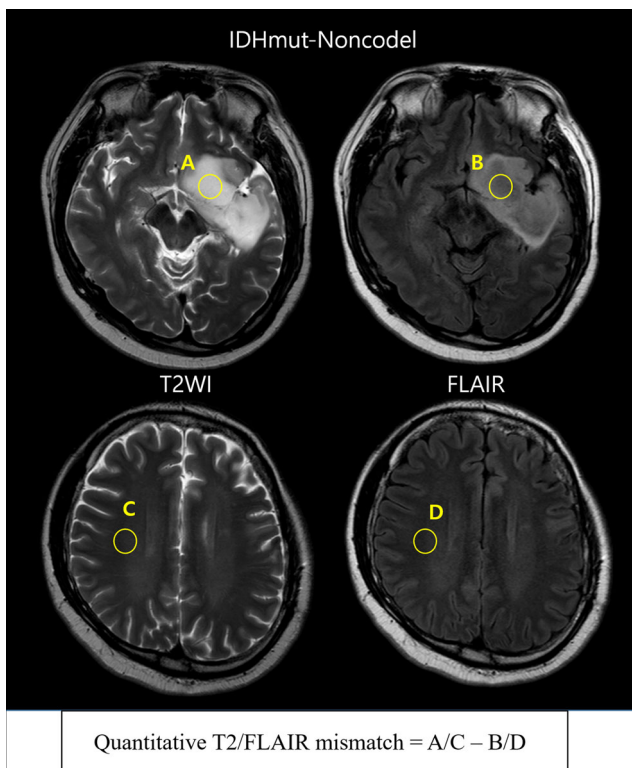


Fig. 4 A grade II glioma with IDHmut-Noncodel shows visual and quantitative T2/FLAIR mismatch sign. ROIs (circle) are drawn on the hyperintense tumour in both T2WI and FLAIR images. Other ROIs (circle) are drawn on the normal-appearing contralateral brain parenchyma. The T2/FLAIR mismatch degree is 2.13

values improve the accuracy of the visual T2/FLAIR mismatch findings in the IDHmut-Noncodel group.

The difference in nCBV between the IDHmut-Noncodel group and other diffuse lower-grade gliomas was not helpful for identifying molecular subtypes. Although the 1p/19q codeletion is associated with a higher CBV [25], the nCBV can be confounded by tumour grades. A previous multivariate analysis that included 64 patients with diffuse lower-grade glioma demonstrated that the CBV does not improve the molecular subclassification [3]. However, we showed that nCBV improved the molecular subclassification by using the combination model. In addition, we showed that nCBV was a significant indicator for distinguishing the IDHmut-Noncodel from other groups on univariate and multivariate logistic regression analyses. Since molecular subtyping outweighs histopathologic grade for predicting the treatment response and survival of patients with diffuse lower-grade gliomas [1, 2], nCBV may become an indicator similar to ADC for the molecular subtyping of diffuse lower-grade gliomas.

The present study had several limitations. First, consensus assignment of the T2/FLAIR mismatch sign may create a pseudo-consensus [26] whereby a dominant radiologist could make the actual decision. We attempted to mitigate this by first

achieving excellent inter-reader agreement ($ICC = 0.89$) before consensus reading. Second, the assignment of an equivocal T2/FLAIR mismatch may seem artifactual; however, it may reflect a real-world situation in which imaging findings are not clear-cut. In our study, we showed the quantitative T2/FLAIR mismatch shows moderate correlation to visual T2/FLAIR mismatch sign, further supporting the imaging phenotype. Third, the IDHmut-Noncodel group included a relatively small number of patients, which may affect positive or negative predictive value of the imaging parameters. A 100% of positive predictive value does not indicate 100% of accuracy as positive or negative predictive values were affected by disease prevalence in study population, not likely so-called diagnostic performance using AUC, sensitivity or specificity. Fourth, the ratio between the IDH mutant and the IDHwt was 13:9, and IDHwt was more frequent than the previously reported studies [4, 17, 27]. The diagnostic performance of imaging parameters is not affected by disease prevalence, which was determined by AUC, sensitivity and specificity [28]. Nonetheless, data imbalance may limit the translation of our results to the general population in terms of disease-specific probability. In the future, further studies with a larger sample size reflecting general disease incidence in diffuse lower-grade gliomas will support our studies.

In conclusion, the combination of the visual T2/FLAIR mismatch sign with ADC or CBV parameters can improve the identification of IDHmut-Noncodel diffuse lower-grade gliomas. This image-based approach incorporating ADC and CBV single parameters with T2/FLAIR mismatch sign could be helpful in analysing unresectable gliomas in eloquent locations or gliomas in patients who cannot be operated on for medical reasons.

Funding This research was supported by the Basic Science Research Program through the National Research Foundation of Korea (NRF) funded by the Ministry of Education, Science and Technology (grant number, NRF-2017R1A2A2A05001217) and by a grant (2017-7030) from the Asan Institute for Life Sciences, Asan Medical Center, Seoul, Korea. The funders had no role in study design, data collection and analysis, decision to publish or preparation of the manuscript.

Compliance with ethical standards

Guarantor The scientific guarantor of this publication is Ho Sung Kim.

Conflict of interest The authors of this manuscript declare no relationships with any companies, whose products or services may be related to the subject matter of the article.

Statistics and biometry One of the authors has significant statistical expertise: Seo Young Park.

Informed consent Written informed consent was waived by the Institutional Review Board.

Ethical approval Institutional Review Board approval was obtained.

Methodology

- retrospective
- cross-sectional study
- performed at one institution

References

1. Brat DJ, Verhaak RG, Aldape KD et al (2015) Comprehensive, integrative genomic analysis of diffuse lower-grade gliomas. *N Engl J Med* 372:2481–2498
2. Eckel-Passow JE, Lachance DH, Molinaro AM et al (2015) Glioma groups based on 1p/19q, IDH, and TERT promoter mutations in tumors. *372:2499–2508*
3. Leu K, Ott GA, Lai A et al (2017) Perfusion and diffusion MRI signatures in histologic and genetic subtypes of WHO grade II–III diffuse gliomas. *J Neurooncol* 134:177–188
4. Patel SH, Poisson LM, Brat DJ et al (2017) T2–FLAIR mismatch, an imaging biomarker for IDH and 1p/19q status in lower-grade gliomas: a TCGA/TCIA project. *Clin Cancer Res* 23:6078–6085
5. van den Bent MJ, Smits M, Kros JM, Chang SM (2017) Diffuse infiltrating oligodendroglioma and astrocytoma. *J Clin Oncol* 35:2394–2401
6. Van den Bent MJ, Looijenga LH, Langenberg K et al (2003) Chromosomal anomalies in oligodendroglial tumors are correlated with clinical features. *Cancer* 97:1276–1284
7. Nobusawa S, Watanabe T, Kleihues P, Ohgaki H (2009) IDH1 mutations as molecular signature and predictive factor of secondary glioblastomas. *Clin Cancer Res* 15:6002–6007
8. Kickingereder P, Sahn F, Radbruch A et al (2015) IDH mutation status is associated with a distinct hypoxia/angiogenesis transcriptome signature which is non-invasively predictable with rCBV imaging in human glioma. *Sci Rep* 5:16238
9. Chen L, Liu M, Bao J et al (2013) The correlation between apparent diffusion coefficient and tumor cellularity in patients: a meta-analysis. *PLoS One* 8:e79008
10. Xing Z, Yang X, She D, Lin Y, Zhang Y, Cao D (2017) Noninvasive assessment of IDH mutational status in World Health Organization grade II and III astrocytomas using DWI and DSC-PWI combined with conventional MR imaging. *AJNR Am J Neuroradiol* 38:1138–1144
11. Coons SW, Johnson PC, Scheithauer BW, Yates AJ, Pearl DK (1997) Improving diagnostic accuracy and interobserver concordance in the classification and grading of primary gliomas. *Cancer* 79:1381–1393
12. van den Bent MJ (2010) Interobserver variation of the histopathological diagnosis in clinical trials on glioma: a clinician's perspective. *Acta Neuropathol* 120:297–304
13. Siegal T (2016) Clinical relevance of prognostic and predictive molecular markers in gliomas. *Adv Tech Stand Neurosurg*. https://doi.org/10.1007/978-3-319-21359-0_4:91-108
14. Lai A, Kharbanda S, Pope WB et al (2011) Evidence for sequenced molecular evolution of IDH1 mutant glioblastoma from a distinct cell of origin. *J Clin Oncol* 29:4482–4490
15. Weisskoff R, Boxerman J, Sorensen A, Kulke S, Campbell T, Rosen B (1994) Simultaneous blood volume and permeability mapping using a single Gd-based contrast injection. *Proceedings of the Society of Magnetic Resonance, Second Annual Meeting*, pp 6–12
16. Boxerman J, Schmainda K, Weisskoff R (2006) Relative cerebral blood volume maps corrected for contrast agent extravasation significantly correlate with glioma tumor grade, whereas uncorrected maps do not. *AJNR Am J Neuroradiol* 27:859–867
17. Broen MP, Smits M, Wijnenga MM et al (2018) The T2-FLAIR mismatch sign as an imaging marker for non-enhancing IDH-mutant, 1p/19q-intact lower-grade glioma: a validation study. *Neuro Oncol* 20:1393–1399
18. Maes F, Collignon A, Vandermeulen D, Marchal G, Suetens P (1997) Multimodality image registration by maximization of mutual information. *IEEE Trans Med Imaging* 16:187–198
19. Chung WJ, Kim HS, Kim N, Choi CG, Kim SJ (2013) Recurrent glioblastoma: optimum area under the curve method derived from dynamic contrast-enhanced T1-weighted perfusion MR imaging. *Radiology* 269:561–568
20. Delgado-López P, Corrales-García E, Martino J, Lastra-Aras E, Dueñas-Polo MT (2017) Diffuse low-grade glioma: a review on the new molecular classification, natural history and current management strategies. *Clin Transl Oncol* 19:931–944
21. Koeller KK, Rushing EJ (2005) Oligodendroglioma and its variants: radiologic-pathologic correlation. *Radiographics* 25:1669–1688
22. Lee S, Choi SH, Ryoo I et al (2015) Evaluation of the microenvironmental heterogeneity in high-grade gliomas with IDH1/2 gene mutation using histogram analysis of diffusion-weighted imaging and dynamic-susceptibility contrast perfusion imaging. *J Neurooncol* 121:141–150
23. Tan WL, Huang WY, Yin B, Xiong J, Wu JS, Geng DY (2014) Can diffusion tensor imaging noninvasively detect IDH1 gene mutations in astroglomas? A retrospective study of 112 cases. *AJNR Am J Neuroradiol* 35:920–927
24. Jenkinson MD, Smith TS, Brodbelt AR, Joyce KA, Warmke PC, Walker C (2007) Apparent diffusion coefficients in oligodendroglial tumors characterized by genotype. *J Magn Reson Imaging* 26:1405–1412
25. Chawla S, Krejza J, Vossough A et al (2013) Differentiation between oligodendroglioma genotypes using dynamic susceptibility contrast perfusion-weighted imaging and proton MR spectroscopy. *AJNR Am J Neuroradiol* 34:1542–1549
26. Bankier AA, Levine D, Halpern EF, Kressel HY (2010) Consensus interpretation in imaging research: is there a better way? *Radiology* 257:14–17
27. Cohen AL, Holmen SL, Colman H (2013) IDH1 and IDH2 mutations in gliomas. *Curr Neurol Neurosci Rep* 13:345
28. Park SH, Han K (2018) Methodologic guide for evaluating clinical performance and effect of artificial intelligence technology for medical diagnosis and prediction. *Radiology* 286:800–809

Publisher's note Springer Nature remains neutral with regard to jurisdictional claims in published maps and institutional affiliations.